A Test of Microtubule Translocation during Neurite Elongation

Soo-Siang Lim,* Kathryn J. Edson,‡ Paul C. Letourneau,‡ and Gary G. Borisy*

*Molecular Biology Laboratory, University of Wisconsin, Madison, Wisconsin 53706; and ‡Department of Cell Biology and Neuroanatomy, University of Minnesota, Minneapolis, Minnesota 55455

Abstract. In a previous study using PC-12 cells (Lim, S. S., P. J. Sammak, and G. G. Borisy. 1989. *J. Cell Biol.* 109:253–263), we presented evidence that the microtubule component of the neuronal cytoskeleton is differentially dynamic but stationary. However, neurites of PC-12 cells grow slowly, hindering a stringent test of slow axonal transport mechanisms under conditions where growth was substantial. We therefore extended our studies to primary cultures of dorsal root ganglion cells where the rate of neurite outgrowth is rapid. Cells were microinjected with X-rhodamine-labeled tubulin 7–16 h after plating. After a further incubation for 6–18 h, the cells were photobleached with an argon ion laser. Using a cooled charged couple device and video microscopy, the cells were monitored for growth of the neurite and movement and recovery of fluorescence in the bleached zone. As for PC-12 cells, all bleached zones in the neurite recovered their fluorescence, indicating that incorporation of tubulin occurred along the neurite. Despite increases in neurite length of up to 70 μm, and periods of observation of up to 5 h, no movement of bleached zones was observed. We conclude that neurite elongation cannot be accounted for by the transport of a microtubule network assembled only at the cell body. Rather, microtubules turn over all along the length of the neurite and neurite elongation occurs by net assembly at the tip.

How is the cytoskeleton assembled in the growing neurite? Cytoskeletal assembly depends on the availability of component units. However, the geometry of neurons complicates this basic requirement. As the sole site of protein synthesis, the cell body is the source of subunits for neurite growth. The progressive growth of neurites away from the cell body and their subsequent maintenance demand that materials be conveyed to distal sites, often over long distances. These conditions necessitate a close coupling of the assembly of the cytoskeleton with transport processes from the cell body.

Consideration of how and in what form tubulin is transported must also take into account the site of microtubule assembly. For example, if assembly occurs only in the cell body, then the transport form would be the microtubule polymer. Assembly elsewhere in the neuron would require that nonpolymeric (unassembled) forms of tubulin be conveyed to distal sites of assembly. Hence, identification of the basic units of transport and their sites of assembly into polymer are essential for understanding the mode of assembly of the neuronal cytoskeleton.

A large body of work (reviewed in 9) suggests that microtubules are the transport form of tubulin in mature, nongrowing neurons. They are thought to be assembled at the cell body, to travel through the axon at 0.5–4 mm/d, and to be degraded at distal sites (2, 4, 12, 13). Consistent with this idea, kinetic studies using pulse-labeled neurons in culture showed that soon after synthesis, the majority of tubulin and neurofilament proteins enter into insoluble forms (3). Further, similarities between the rate of transport of cytoskeletal proteins and the growth of regenerating neurites led to the suggestion that movement en masse of preexisting microtubules and intermediate filaments may be the limiting process critical in the mechanism of neurite elongation (reviewed in 7).

Alternatively, the protein molecules themselves or nonmicrotubule oligomers could be the units of transport (1, 27, 28). Depending on the site(s) of assembly, two possible mechanisms could give rise to neurite elongation. If the growth cone was the major site of microtubule assembly (1), local assembly of microtubules from tubulin molecules transported to this region would allow for neurite growth. If microtubules were able to incorporate subunits at all distal ends throughout the neuron (18) but were differentially dynamic (16), microtubule turnover would occur throughout, but neurite elongation could result from some mechanism(s) that promotes net assembly of microtubules at the tip.

The presence or absence of microtubule polymer transport and the identification of sites of microtubule assembly are criteria that will distinguish between the various possibilities outlined above. Information concerning both microtubule movement and sites of assembly can be obtained by combining the techniques of microinjection of labeled tubulin and fluorescence recovery after photobleaching. Using similar techniques, Keith (10) reported distal translocation of bleached zones at rates similar to slow axonal transport. No information was presented with regard to the recovery of bleached zones. In contrast, our experiments in PC-12 cells (16) indicated that bleached zones do not move but do re-

© The Rockefeller University Press, 0021-9525/90/07/123/8 $2.00

cover their fluorescence. These observations suggest that microtubules in the neuron are stationary and that microtubule assembly occurs throughout the neuron.

Since neurites of PC-12 cells grow slowly, recovery of fluorescence in the bleached zones occurred before we could document substantial elongation. Hence we were not able to test definitively whether polymer transport and neuronal elongation were coupled events. Therefore we extended our studies to primary cultures of dorsal root ganglion cells, where neurite growth is rapid. We report here that despite significant increases in neurite length, no movement of bleached zones was observed, indicating that neurite elongation cannot be accounted for by the transport of a microtubule network assembled only at the cell body. During neurite elongation, all bleached zones in the neurite recovered their fluorescence and the increase in length of the neurite corresponded to the increase in the length of the distal-most segment. We conclude that steady state turnover of microtubules occurs along the length of the neurite and that neurite elongation is accompanied by net assembly of microtubules at the tip.

Materials and Methods

Cell Culture

Cultures of sensory neurons were prepared from chick dorsal root ganglia as previously described (14). For ease of locating injected cells, the coverslips were carbon coated to produce a locater pattern (16). Once plated onto the coverslips, the cells were allowed to settle for 9–12 h before microinjection.

Microinjection

X-rhodamine labeling of tubulin was performed as previously described (21). Just before use, an aliquot of x-rhodamine tubulin was thawed and spun at 20,000 *g* for 30 min to remove particulates. To ensure maximal incorporation of the labeled tubulin into microtubules, cells without neurites or with newly sprouting neurites were selected for microinjection. Injected volumes were estimated by eye to be <10% of the volume at the cell body as no discernible distortion of the membrane was observed.

Photobleaching

The photobleaching apparatus was assembled as described before (16). The maximum laser intensity at the specimen as measured directly using an optometer (model 370; United Detector Technology, Hawthorne, CA) was 60 MW/m^2. This exposure (60 $MW/m^2 \times 300$ ms = 18 MJ/m^2) was eightfold less than the exposure (71 $MW/m^2 \times 2$ s = 142 MJ/m^2) reported to cause dissolution of microtubules in vitro (26).

Microinjected cells were allowed to equilibrate with the labeled tubulin for 6–18 h before photobleaching. An injected cell was selected and then photobleached once on the primary neurite. Phase-contrast images and fluorescent images were taken before and after photobleaching to record the progress of the cell during recovery of the bleached zones.

Image Acquisition and Display

To prevent excessive irradiation, cells were observed by fluorescence only at intervals of 20–90 min. The microscope was equipped with a 25× objective, illuminated with a 100 W mercury arc lamp, and the light passed through ultraviolet and infrared blocking filters, neutral density filters, and a wide-band Zeiss rhodamine filter set. Cells were focused with the aid of a SIT TV camera (Dage-MTI, Inc. Michigan City, IN) and an image processor (Quantex Corp., Sunnyvale, CA). A charged couple device (CCD), attached to the side port of the microscope with a 5× ocular and a Tokina 80-200 zoom photographic lens, was used to collect both fluorescent and phase images. This series 200 CCD camera (PhotoMetrics Ltd., Tucson, AZ) contained a 384 × 576 pixel chip (Thompson CSF TH7882CDA) that was thermoelectrically cooled to −50°C to reduce the dark current noise and images were digitized to 14-bit depth. After temporary storage on the hard drive of a personal computer (AST premium/386; Irvine, CA), digital image files from the CCD were archived on a WORM drive optical disc (model 3363; IBM Corp.). During experiments, all images were documented with a video printer (P-60U; Mitsubishi Corp.). Publication quality photographs were subsequently produced from a high resolution black and white monitor (Sierra Scientific, Mountain View, CA) on Technical Pan 2415 film.

Data Analysis

Measurements of fluorescence intensity along neurites were made from images that were corrected for background noise, camera-related variation in illumination (flat-fielding), and bleaching during image acquisition. Fluorescence recovery after photobleaching was assayed by determining the ratio of the radiance in the bleached zone to that in adjacent regions. Measurement of the position of a bleached zone was made relative to the cell body, branch points, and other landmark features in the images. Measurements of neurite growth were taken during the times that bleached zones were still discernible.

Indirect Immunofluorescence Microscopy

Dorsal root ganglion cells were processed for indirect immunofluorescence as previously described (16). The antitubulin antibody was purchased from Accurate Chemical & Scientific Corp. (Westbury, NY).

Results

Microtubules Are Not Broken by Photobleaching

For a marker protein to report faithfully on the behavior of microtubules in vivo, it is important that it becomes incorporated into the cytoskeleton without significantly perturbing dynamics or neurite extension, and also, that subsequent experimental manipulations (especially photobleaching) do not disrupt the microtubules. To ensure that the labeled tubulin was uniformly incorporated into the microtubule cytoskeleton, cells were microinjected before neurite extension and allowed to incubate for a further 8–16 h after microinjection. Fig. 1, *a–c* are live images of a cell that was microinjected with X-rhodamine tubulin. Comparison of the phase image (Fig. 1 *a*) with the fluorescent image (*b*) indicated that only the cell that was microinjected was fluorescent. Immediately after photobleaching, a postbleach image was captured (Fig. 1 *c*), and the cells lysed, fixed, and processed for antitubulin immunofluorescence.

After a lysis treatment to remove soluble material, the cell in Fig. 1, *a–c* retained its fluorescence except for the region of the bleached zone (*d*). This confirmed that the labeled rhodamine tubulin was incorporated into a detergent-lysis-resistant form, presumably microtubules. The antitubulin immunofluorescence reactivity visible in the fluorescein channel (Fig. 1 *e*) was continuous through the bleached zone. This indicated that under the experimental conditions used, microtubules were not broken by the photobleaching. In addition to the cell shown above (fixed 25 min after photobleaching) cells were lysed and fixed at various other time points after photobleaching to assay for damage that may not have been immediately apparent after photobleaching (26). Neuronal cells lysed and fixed from 1–60 min postbleach all showed continuity of antitubulin immunofluorescence through the bleached zone and we conclude that they did not suffer any visible damage from the photobleaching. In addition, the growth rate of neurites in the experimental cells fell within the range of growth of control cells (15–50 μm/h).

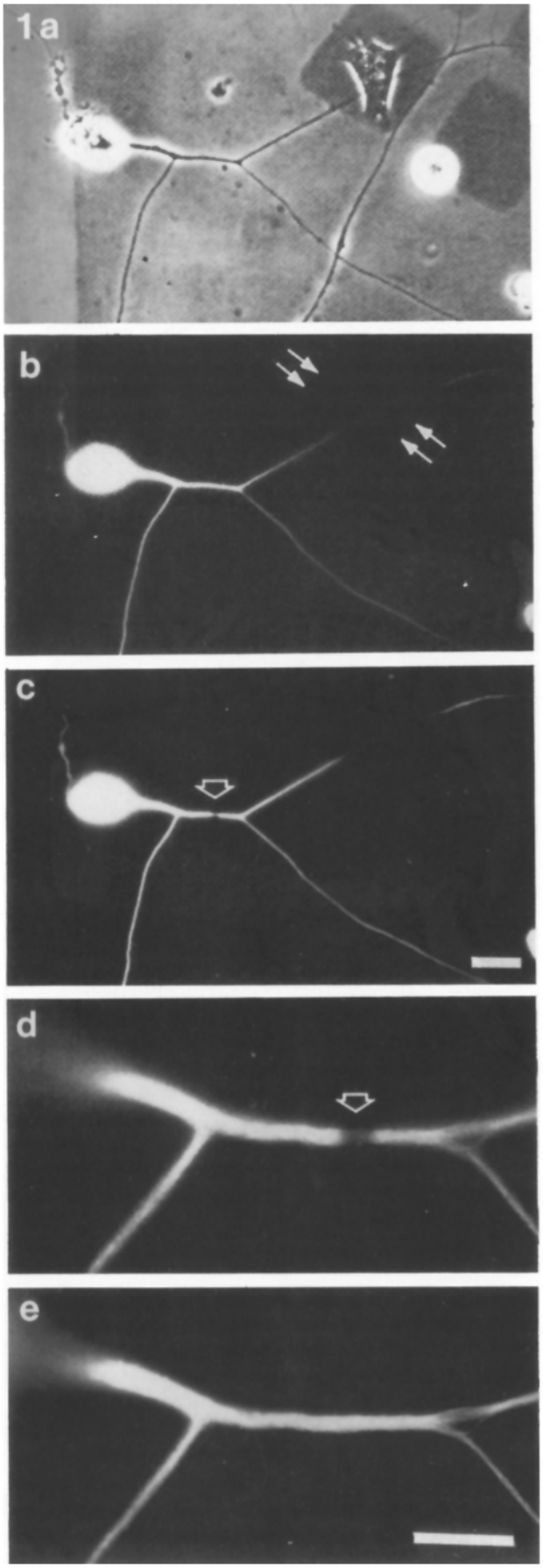

Microtubules Remain Stationary during Neurite Outgrowth

The rate of transport of microtubules was assayed by monitoring the position of bleached zones over a period of time. Bleached zones disappeared eventually because of microtubule turnover. Fig. 2 shows direct fluorescent micrographs of a bipolar cell bleached on the larger neurite shaft and observed for 240 min. Elongation of the neurite shaft was clearly evident, but the position of the bleached zone remained constant relative to the cell body. Initially 110 μm in length at the time of photobleaching, the neurite grew an additional 45 μm by the last time point at which the bleached zone was still visible (142 min; Fig. 2 *f*). It continued to grow such that at 240 min after photobleaching, the total increase in length of the neurite was 80 μm (Fig. 2 *g*).

In a pseudounipolar cell with multiple branches (Fig. 3, *a* and *b*), a bleached zone was placed on the primary trunk of the neurite shaft (*c*). At 53, 143, and 275 min after photobleaching, fluorescence images (Fig. 3, *d'*, *e'*, *f'*) were taken to assess both the position of the bleached zone and its fluorescence intensity. Corresponding phase images were also taken at the same time points to monitor growth of all neuritic branches. No significant movement of the bleached zone was observed throughout this time period although the two distal branches shown in Fig. 3, *d–f* had each elongated by 35 and 37 μm and the combined increase in length of all four distal branches added up to ~172 μm.

Neurite Growth Occurs by Increase in Length at Distal Ends

A comparison of the bleached zone–cell body distances and the bleached zone–growth cone distances indicated no change in the former while the latter increased with neurite elongation. This indicates that during neurite elongation, net assembly of microtubules occurs at the distal end. Morphological analyses of the growth pattern of dorsal root ganglion

Figure 1. Microtubules are continuous through bleached zones. About 8–16 h after microinjection with X-rhodamine-tubulin, a small region of dorsal root ganglia neurites was photobleached. 25 min after photobleaching, this cell was lysed and fixed and subsequently processed for indirect immunofluorescence microscopy using an antitubulin antibody (YL1/2) and a FITC-conjugated anti-rat secondary antibody. (*a–c*) Live images of the cell before photobleaching (*a* and *b*) and immediately after photobleaching (*c*). Comparison of the phase image in *a* and the fluorescent images (*b* and *c*) indicates that only the injected cell is fluorescent. The carbon-coated grid pattern on the coverslips provided a reference framework for relocating and identifying injected cells as well as for monitoring their subsequent growth. However, the carbon-coated regions also serve as neutral density filters that diminish the fluorescence intensity of overlying structures (*arrows* in *b*). To avoid ambiguity, only regions of neurites on carbon-free areas were selected for photobleaching. After lysis and fixation, the direct rhodamine fluorescence image (*d*) indicates X-rhodamine-tubulin to be incorporated into neuritic microtubules. Fluorescence is continuous along the neurite except at the bleached zone (*arrowhead*). The corresponding image in the fluorescein channel indicates that the anti-tubulin staining is continuous through the bleached zone. Microtubules in the bleached zone remain intact after photobleaching. Bars: (*a–c*) 20 μm; (*d*) 10 μm.

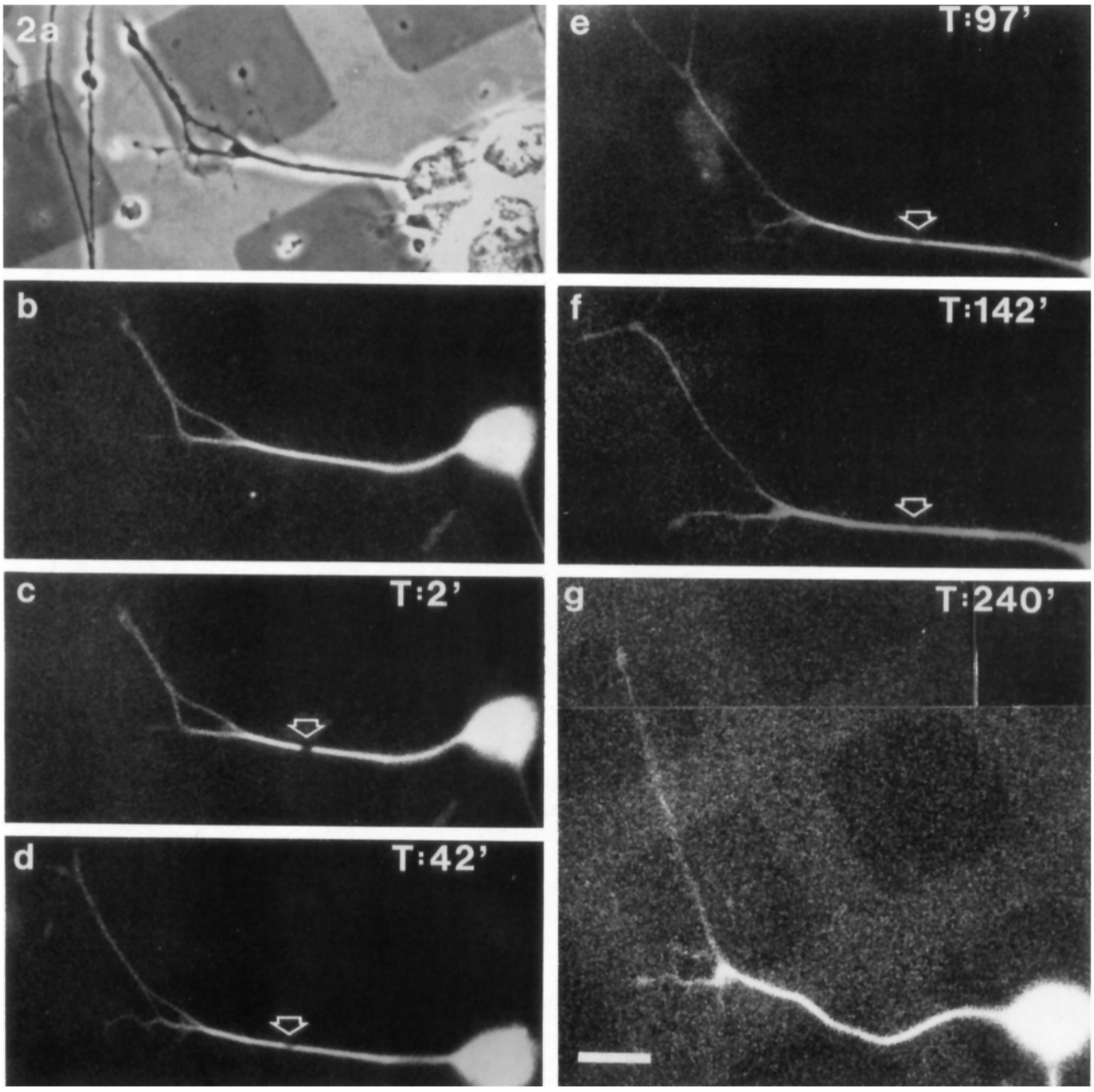

Figure 2. Microtubules remain stationary during neurite growth: a bipolar cell. Before photobleaching, the fluorescent image (*b*) identified the injected cell from neighboring cells as observed in the phase image (*a*). (*c–g*) Fluorescent images captured after photobleaching and the time after photobleaching is indicated by *T* in minutes. During the period that the bleached zone in this cell is still detectable (2.5 h, *c–f*), no obvious change in its location is observed despite a significant increase in neurite length. This cell has remained healthy after the experimental manipulations and continued to grow (*g*). Unfortunately, attempts to remove debris in the field of view also dislodged the proximal neurite slightly. Bar, 20 μm.

cells reinforce this conclusion. The cell in Fig. 3 was analyzed for the increase in length of the various branched segments according to the procedure of Bray (5). Fig. 4 *a* is a diagrammatic reconstruction of the cell at various time points, the cell being divided into various segments corresponding to the different neuritic branches. As is apparent in Fig. 4 *a* and confirmed in *b*, proximal segments showed no significant changes in length even though the overall dimensions of the cell had increased. As previously reported in superior cervical ganglion cells (5), only the distal-most segments contribute to the increase in neurite length.

Quantitative Assessment of Movement and Turnover of Bleached Zones

Bleached zones were placed at varying distances from the cell body and the data obtained from different cells was normalized as relative movement of the bleached zone with re-

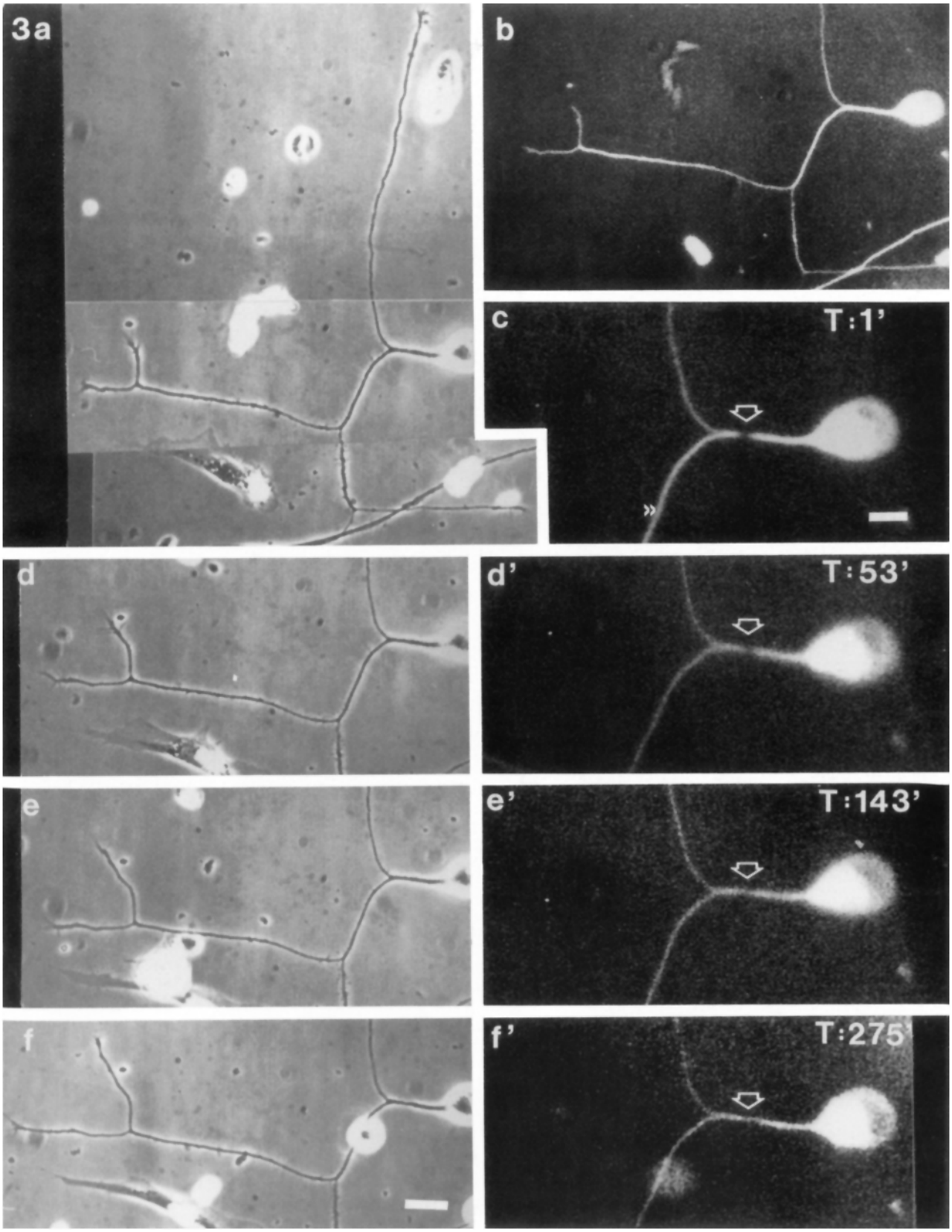

Figure 3. Microtubules remain stationary during neurite growth: a pseudounipolar cell with multiple branches. With this large cell, montages of phase images were constructed to record the lengths of the various neuritic branches (*a*). To avoid excessive irradiation of the cell, fluorescent images (*b*, *c'–f'*) were taken only in the field of view of the bleached zone. (*a* and *b*) Images taken before photobleaching. The time after photobleaching for postbleached images are indicated by *T*. For each time point, paired phase and fluorescent images (*d*, *d'*, and *e*, *e'*, and *f*, *f'*) reveal changes in length of the neurite and the position of the bleached zone (*arrowhead*). Bar, 20 μm.

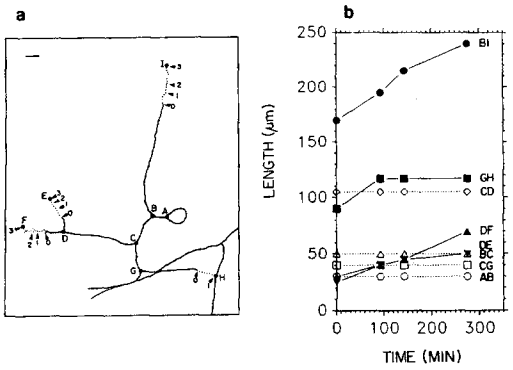

Figure 4. Neurite growth occurs by addition in length at distal ends. (*a*) A diagrammatic representation of the same cell in Fig. 3, drawn to scale (bar, 20 μm). The cell is divided into segments corresponding to the various neuritic branches. *O* indicates the length of the segment before photobleaching. At various time points after photobleaching (1 = 93 min; 2 = 143 min; 3 = 275 min), measurements of the segments were made from montages of phase images. *b* shows changes in lengths of the neuritic segments at the time points indicated in Fig. 3 *a*. Distalmost segments (*BI*, *DE*, *DF*, and *GH*) show increases in lengths while more proximal segments do not show change.

spect to its position at the time of photobleaching. For observation periods of up to 4.5 h (limited by the recovery of the bleached zone), no obvious unidirectional movement of the bleached zones, as predicted by slow axonal transport (Fig. 5, *dashed line*), was observed. Analysis of 10 bleached zones in 10 cells is plotted in Fig. 5 *a*. Although we only show data for bleached zones placed on primary neurites, zones placed on secondary or tertiary branches also did not move.

In Fig. 5 *b*, relative movement of bleached zones is plotted against growth increments of neurites (>20 μm). Despite increases of up to 70 μm, a corresponding translocation of the bleached zones (Fig. 5 *b*, *dashed line*) was not observed. We conclude that the microtubule component of the neuronal cytoskeleton is stationary, and that neurite elongation cannot be attributed to polymer transport.

However, quantitation of fluorescence recovery after photobleaching indicates that the neuronal microtubules turnover (Fig. 6). Since diffusion of the tubulin dimer ($D \sim 10^{-8}$ $cm^2 \cdot s^{-1}$) across the bleached zone would be expected to occur within seconds, the low level of fluorescence in the first postbleach image (2 min) indicates that the pool of soluble tubulin in the neurite is small. The time course of recovery indicates that microtubules in the neurite shaft turnover slowly ($t_{1/2}$ 1–2 h). The maintenance of the symmetry and width of the intensity distribution indicates that recovery does not occur by movement of microtubules proximal to the bleached zone.

Discussion

Stationary Bleached Zones Indicate Lack of Polymer Transport

The principal observation of this study is that bleached zones placed on neurite shafts failed to move despite significant increases in neurite length. Our evidence argues that neuronal microtubules are stationary and that neurite elongation is not dependent on polymer transport from the cell body. These results are contrary to the predictions of the current models of slow axonal transport and their implications for microtubule assembly and neurite growth. What are the experimental pitfalls and limits of the photobleaching experiments?

The effects of irradiation from photobleaching and live observations of cells using fluorescence microscopy have been a concern of this laboratory and others. Vigers et al. (26) have reported that fluorescent microtubules appear to break up under illumination. Using a conservative dose of irradiation in this study (Materials and Methods) and others, we did not see evidence of microtubule damage at both light and EM levels (6, 16, 20, 21). In addition, a recent study using correlative light and low voltage scanning electron microscopy designed specifically to address photodamage confirmed the integrity of microtubules when exposed to the light energy levels of our experimental conditions (Centonze, V. E., and

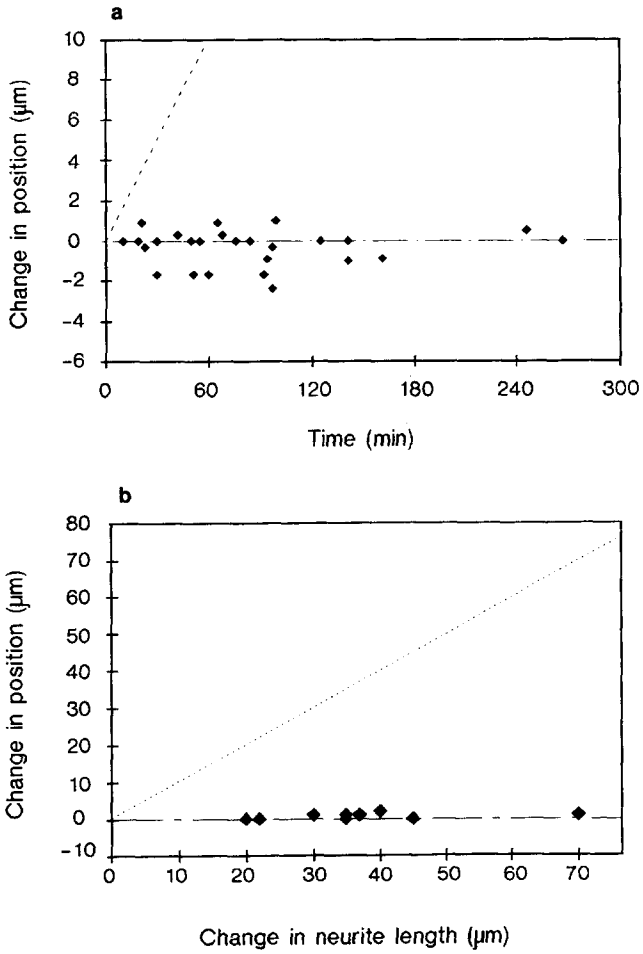

Figure 5. Quantitative assessment of the movement of bleached zones. (*a*) The change in distance between the bleached zone and the cell body is plotted as a function of time. The precision of each measurement was +/− 1 μm. For comparison, the minimal rate of slow axonal transport is ~0.25 mm/d or 10 μm/h (*dashed line*). (*b*) The change in distance between the bleached zone and the cell body is plotted against the increases in neurite length. The precision of each measurement was +/− 1 μm. For comparison, the rate of polymer displacement needed for corresponding neurite growth is plotted (*dashed line*).

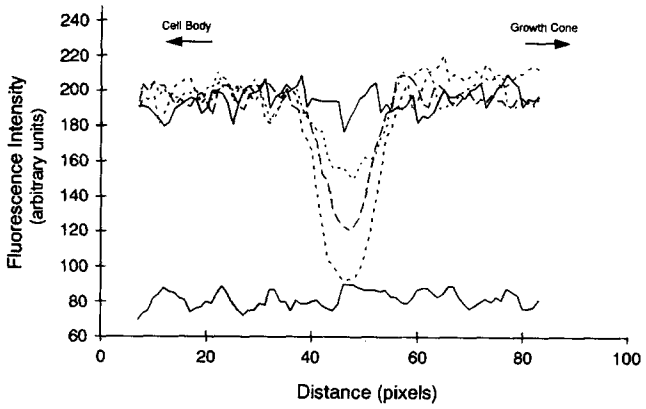

Figure 6. Quantitation of fluorescence recovery in bleached zones. The cell in Fig. 2 is used in this example of fluorescence intensity measurements across the region of the bleached zone. The intensity profile shows fluctuations along the length of the neurite both before (*upper solid line*) and after (*dashed lines*) photobleaching. Photobleaching (see Fig. 2 *c*) reduced fluorescence intensity in the bleached zone close to background levels (*lower solid line*). At 42 (see Fig. 2 *d*) and 142 min (see Fig. 2 *f*) after photobleaching, fluorescence levels increased resulting in a more shallow trough in the intensity profiles (*dashed line*). The overall shape and symmetry of the trough remained unchanged. 1.8 pixels = 1 μm.

G. G. Borisy, unpublished results). Furthermore, cell function appears unperturbed, as evidenced by normal rates of neurite elongation in this study and normal progression of mitosis (6).

The photobleaching experiments are limited by the extent of photobleaching, the intensity of fluorescence in the recorded images, and the recovery of fluorescence after photobleaching. Although we have not attempted to determine the precise relationship between fluorescence intensity and microtubule concentration, it is reasonable to assume that above a value equal to the subunit contribution, the fluorescence intensity would be proportional to the amount of microtubule polymer at a given position in the neurite. Because the CCD image sensor is a linearly responding, quantitative device, a comparison of the fluorescence in the bleached zone and flanking regions would reveal whether a subset of the microtubules were moving. If polymer sliding occurs in neurons (11) and if 50% of the microtubules were stationary and 50% moved, we would expect first a broadening of the bleached zone and then a splitting into two equal components. This was clearly not observed. We estimate that we would not have been able to detect a moving subset of 10–20% of the microtubules, but the results do permit us to say that the bulk of the microtubules must be stationary.

Microtubule Turnover along the Length Is Consistent with Transport of Nonpolymeric Tubulin

Since we did not observe any polymer transport, we conclude that neurite growth must be due to the transport of tubulin in an unassembled state such as tubulin dimer or a form of nonmicrotubule polymer (27, 28). Fluorescence recovery of bleached zones results from the assembly of new microtubule domains all along the length. In this and a previous study (15), we showed that the rate of microtubule turnover in neuronal cells is relatively slow when compared with similar studies in nonneuronal cells (21, 23–25).

The occurrence of microtubule turnover throughout the neuron (16, 18) argues that there is no specific cellular site of assembly but rather, microtubule assembly is dictated by the presence of free ends. Axonal microtubules show polarity such that their plus (+) ends are distal to the cell body (8). Okabe and Hirokawa (18) provided ultrastructural evidence that labeled tubulin microinjected into neuronal cells can move unimpeded into the neurite and become incorporated at the distal, plus ends of individual microtubules. This end-mediated assembly, and the time-dependent increase in length of the labeled domains is similar to results of studies in nonneuronal cells (24, 25) which have been interpreted in terms of the dynamic instability model of microtubule turnover (17, 22).

Net Assembly of Microtubules at the Growth Cone

Our phase microscopic analysis of growing DRG cells confirms the study of Bray (5) that elongation of neurites can be accounted for entirely by an increase in length of the distal-most segment. In addition, our fluorescence and photobleaching analysis indicates that the microtubule component of the neuronal cytoskeleton in these same cells is stationary. The syllogistic inference to be drawn from these statements is that during neurite elongation net microtubule assembly takes place at the distal tip. In a previous study, we found microtubule turnover to be faster in the growth cone than in the neurite shaft (16). Other observations consistent with the growth cone being a major site of microtubule assembly are the predominance of free microtubule ends at the growth cone (15), the heightened sensitivity of neurite elongation to microtubule depolymerizing drugs when applied to the growth cone than when applied to the cell body or neurite shaft (1), and the lack of posttranslationally modified tubulin characteristically associated with microtubule stability (16, 19).

We conclude that neurite elongation is not dependent on bulk translocation of microtubules previously assembled at the cell body. Neuronal microtubules are dynamic and subunit exchange occurs throughout the cell, accounting for microtubule turnover at steady state. Under conditions of neurite extension, we infer that net assembly of microtubules occurs at the distal tip.

We thank John Peloquin for the preparation of the X-rhodamine-tubulin, Dr. Paul Kronebusch for making the laser beam power measurements, and Steve Limbach and Leanne Olds for expert illustration. We are also grateful to Dr. John Fallon (Department of Anatomy, University of Wisconsin) for the use of the egg incubator throughout the course of this study.

This work was supported by National Institutes of Health grants GM25062 to G. G. Borisy and H219950 to P. C. Letourneau.

Received for publication October 11, 1989 and in revised form 9 February 1990.

Note Added in Proof: A recent publication by S. Okabe and N. Hirokawa (*Nature (Lond.)*. 1990. 343:479–481) using a similar experimental approach also concluded that microtubules are dynamic and that their translocation does not occur during neurite elongation.

References

1. Bamburg, J. R., D. Bray, and K. Chapman. 1986. Assembly of microtubules at tips of growing axons. *Nature (Lond.)*. 321:788–790.
2. Black, M. M., and R. J. Lasek. 1980. Slow components of axonal transport: two cytoskeletal networks. *J. Cell Biol.* 86:616–623.
3. Black, M. M., P. Keyser, and E. Sobel. 1986. Interval between the synthe-

sis and assembly of cytoskeletal proteins in cultured neurons. *J. Neurosci.* 6:1004–1012.
4. Brady, S. T., and R. J. Lasek. 1982. The slow components of axonal transport: movements, compositions, and organisation. *In* Axoplasmic Transport. D. Weiss, editor. Springer-Verlag, Berlin. 207–217.
5. Bray, D. 1973. Branching patterns of individual sympathetic neurons in culture. *J. Cell Biol.* 56:702–712.
6. Gorbsky, G. J., and G. G. Borisy. 1986. Microtubules of the kinetochore fiber turn over in metaphase but not in anaphase. *J. Cell Biol.* 109:653–662.
7. Grafstein, B., and D. S. Forman. 1980. Intracellular transport in neurons. *Physiol. Rev.* 60:1167–1285.
8. Heidemann, S. R., J. M. Landers, and M. A. Hamborg. 1981. Polarity orientation of axonal microtubules. *J. Cell Biol.* 91:661–665.
9. Hollenbeck, P. J. 1989. The transport and assembly of the axonal cytoskeleton. *J. Cell Biol.* 108:223–227.
10. Keith, C. H. 1987. Slow transport of tubulin in the neurites of differentiated PC12 cells. *Science (Wash. DC).* 235:337–339.
11. Lasek. R. J. 1986. Polymer sliding in axons. *J. Cell Sci. Suppl.* 5:161–179.
12. Lasek, R. J., and S. T. Brady. 1981. The structural hypothesis of axonal transport: two classes of moving elements. *In* Axoplasmic Transport. D. G. Weiss, editor. Springer-Verlag, Berlin. 397–405.
13. Lasek, R. J., and P. N. Hoffman. 1976. The neuronal cytoskeleton, axonal transport and axonal growth. *In* Cell Motility, Cold Spring Harbor Symp. Cell Proliferation. Vol. 3. R. Goldman, T. Pollard, and J. Rosenbaum, editors. Cold Spring Harbor Laboratory, Cold Spring Harbor, NY. 1021–1049.
14. Letourneau, P. C. 1975. Possible roles for cell to substratum adhesion and neuronal morphogenesis. *Dev. Biol.* 44:77–91.
15. Letourneau, P. C. 1982. Analysis of microtubule number and length in cytoskeletons of cultured chick sensory neurons. *J. Neurosci.* 2:806–814.
16. Lim, S. S., P. J. Sammak, and G. G. Borisy. 1989. Progressive and spatially differentiated stability of microtubules in developing neuronal cells. *J. Cell Biol.* 109:253–263.
17. Mitchison, T., and M. Kirschner. 1984. Dynamic instability of microtubule growth. *Nature (Lond.).* 312:237–242.
18. Okabe, S., and N. Hirokawa. 1988. Microtubule dynamics in nerve cells: analysis using microinjection of biotinylated tubulin into PC12 cells. *J. Cell Biol.* 107:651–664.
19. Robson, S. J., and R. D. Burgoyne. 1989. Differential localisation of tyrosinated, detyrosinated, and acetylated alpha-tubulins in neurites and growth cones of dorsal root ganglion neurons. *Cell Motil. Cytoskeleton.* 12:293–282.
20. Sammak, P. J., and G. G. Borisy. 1988. Direct observations of microtubule dynamics in living cells. *Nature (Lond.).* 332:742–726.
21. Sammak, P. J., and G. G. Borisy. 1988. Detection of single fluorescent microtubules and methods for determining their dynamics in living cells. *Cell Motil. Cytoskeleton.* 10:237–245.
22. Sammak, P. J., G. J. Gorbsky, and G. G. Borisy. 1987. Microtubule dynamics in vivo; a test of mechanisms of turnover. *J. Cell Biol.* 104:395–405.
23. Saxton, W. M., D. L. Stemple, R. J. Leslie, E. D. Salmon, M. Zavortink, and J. R. McIntosh. 1984. Tubulin dynamics in cultured mammalian cells. *J. Cell Biol.* 99:2175–2186.
24. Schultze, E., and M. Kirschner. 1986. Microtubule dynamics in interphase cells. *J. Cell Biol.* 102:1020–1031.
25. Soltys, B., and G. G. Borisy. 1985. Polymerization of tubulin in vivo: direct evidence for assembly onto microtubule ends and from centrosomes. *J. Cell Biol.* 100:1682–1689.
26. Vigers, G. P. A., M. Coue, and J. R. McIntosh. 1988. Fluorescent microtubules break up under illumination. *J. Cell Biol.* 107:1011–1024.
27. Weisenberg, R. C., B. Gao, S. Awodi, and J. Flynn. 1987. Microtubule gelation-contraction in vitro and slow axonal transport. *In* Axonal Transport. R. Smith and M. Bisby, editors. Alan R. Liss, Inc., New York. 165–174.
28. Weisenberg, R. C., J. Flynn, B. Gao, S. Awodi, F. Skee, S. R. Goodman, and B. M. Riederer. 1987. Microtubule gelation-contraction: essential components and relation to slow axonal transport. *Science (Wash. DC).* 238:1119–1122.